The Higgs in the sky: production of gravitational waves during a first order phase transition

C. Delaunay[a]*, C. Grojean[a,b]†, G. Servant[a,b]‡

[a] *Service de Physique Théorique, CEA Saclay, F91191 Gif–sur–Yvette, France*

[b] *CERN, theory Division, CH-1211 Geneva 23, Switzerland*

Abstract

If there was a first order phase transition in the early universe, there should be an associated stochastic background of gravitational waves. The characteristic frequency of the spectrum due to phase transitions which took place at the weak scale is precisely in the window that will be probed by LISA. Taking into account the astrophysical foreground, we determine the type of phase transitions which could be detected either at LISA, LIGO or BBO (Big Bang Observer, the 2nd generation of space interferometers), in terms of the amount of supercooling and the duration of the phase transition that are needed. Those two quantities can be calculated for any given effective scalar potential describing the phase transition. In particular, the new models of electroweak symmetry breaking which have been proposed in the last few years typically have a different Higgs potential from the Standard Model. They could lead to a gravitational wave signature in the milli-Hertz frequency, which is precisely the peak sensitivity of LISA. *Talk given by C. Grojean at Quarks 2006, Repino, Russia and at SUSY'06, Irvine, USA. Based on Ref. [1].*

1 Introduction

The weakness of the interaction with matter is a major obstacle for detection of gravitational waves (GW) but it also has the virtue that the information they carry about the state of the universe at the moment of their production has been unaltered. Thus, they are a direct probe of physical processes that took place in the very early universe. Possible cosmological sources of GW include: inflation, preheating, vibration of cosmic strings, preheating, dynamics of extra dimensions, first-order phase transitions... (for a short review, see [2]).

The relic GW background from first-order phase transitions encodes useful information on these major symmetry-breaking events which took place in the early universe. In contrast with the inflationary spectrum, the spectrum is not flat, with a characteristic peak related to the temperature at which the phase transition (PT) took place. This signal can actually be higher by several orders of magnitude than the signal expected from inflation and in some cases can entirely screen it. One symmetry-breaking event which for sure took place in the early universe is electroweak (EW) symmetry breaking. What we do not know yet is whether it was a first order phase transition, in which case it proceeded through nucleation of bubbles resulting in a large departure from thermal equilibrium. Bubble collision and associated motions in the primordial plasma are sources of gravitational waves. The characteristic frequency of the signal is close to the Hubble frequency at the time of the transition $H(T_{EW}) \sim 10^{-14}$ GeV. Once redshifted to today, this corresponds to mHz frequencies, which is precisely the frequency band that LISA is

*e-mail: Cedric.Delaunay@cea.fr

†e-mail: Christophe.Grojean@cern.ch

‡e-mail: Geraldine.Servant@cern.ch

sensitive to (see Fig. 1). It is therefore very exciting that LISA could help providing information on the EW scale, in particular on the nature of the EWPT. It could allow to study the dynamics of the phase transition, which is quite important to analyze models of EW baryogenesis.

The GW spectrum resulting from first order PT was computed in the early nineties [3] but this topic has not received much subsequent attention, as it was found out that there is no first order EWPT in the Standard Model given the experimental bound on the Higgs mass [4]. It was realized ten years after the original calculation that turbulence in the plasma could be a significant source of GW in addition to bubble collisions [5]. Subsequently, the authors of [6] studied the GW signal due to a first order EWPT in the Minimal Supersymmetric Standard Model (MSSM) and its NMSSM extension. Finally, Nicolis [7] did a model-independent analysis for the detectability of GW with LISA.

We believe that it is time to revisit this question for two reasons: The nature of the EWPT will start to be probed experimentally at the LHC. Indeed, it depends essentially on the Higgs sector of the theory or any alternative dynamics for EW symmetry breaking. In the last few years, new models of EW symmetry breaking have been suggested (little higgs, gauge-higgs unification, composite higgs, higgsless models ...) and the nature (smooth cross-over or first-order) of the EWPT in these new frameworks remains unknown. Second, the technology for gravitational wave detectors has made advances and we think it is timely to redo a model-independent analysis not only for LISA but also other devices. GW detectors could then bring information on EW physics complementary to collider data.

2 Astrophysical versus cosmological GW background

Searching for GW waves of cosmological origin is an ambitious goal. Indeed, there is a huge foreground due to astrophysical sources which in principle makes detection impractical if it were not substractable. First the signals from every merging neutron star and stellar mass black holes should be identified and substracted, the primary sources of foreground signals are then galactic and extragalactic binaries. The galactic background produced by binary stars in the Milky Way is many times larger in amplitude than both the extragalactic foreground and LISA's design sensitivity. However, it can be substracted because of its anisotropy, being mostly concentrated in the galactic plane. Irreducible background comes from extragalactic binary stars and is dominated by emission from white dwarves (WD) pairs.

The cosmological GW background due to early universe events is stochastic as the signal comes from the superposition of incoherent sources originating from a huge number of different horizon volumes. For instance, the size of the horizon at the time of the electroweak phase transition was much smaller than today $(10^{-14}\ \mathrm{GeV})^{-1}$, corresponding to a tiny fraction of degree on the sky today. By their very nature, stochastic GW are indistinguishable from the detector noise. Ground-based detectors look for them by coordinated measurements (comparing outputs of multiple detectors to find sources of correlated noise) while LISA can extract the instrumental noise power by combining the signals from its three spacecrafts. The cosmological GW background is discussed in terms of his contribution to the universe's energy density, over some frequency band:

$$\Omega_{GW}(f) = \frac{1}{\rho_{\mathrm{crit}}} \frac{d\rho_{GW}}{d\ln f}. \tag{1}$$

3 A two parameter problem

A first-order phase transition proceeds by nucleation of bubbles. The kinetic energy of bubbles is transferred to GW either by *(i)* bubble collisions or *(ii)* injection of energy into the plasma fluid, creating a homegeneous isotropic fully developed and stationary turbulent regime. In any case, to create a large amount of GW, large masses have to move rapidly, therefore the phase

transition has to proceed in a detonation regime where bubble walls propagate faster than the speed of sound.

The GW background is controlled by two quantities:

$$\alpha \sim \frac{\text{false vacuum energy density = latent heat}}{\text{plasma thermal energy density}}. \tag{2}$$

$$\beta \sim \text{rate of time variation of the nucleation rate} \sim (\text{duration of transition})^{-1}. \tag{3}$$

β fixes the characteristic scale in the problem, the size of bubbles at the time of the collision, and therefore the characteristic frequency f_*. The duration of the phase transition is given by β^{-1} and the size of bubbles is typically $R_b \sim v_b \beta^{-1}$ where v_b is the velocity of the bubble wall. The initial size of the bubble at the time of nucleation (of the order of T^{-1}) is negligible compared to β^{-1} which is of the order of the horizon size.

The parameters α and β can be computed once we know the effective action for nucleating bubbles ("critical bubbles") which can be computed for any scalar potential describing the phase transition, though the numerical computation is rather delicate. The critical bubbles extremize the euclidean action

$$S_3 = \int 4\pi r^2 dr \left(\frac{1}{2} \left(\frac{d\phi_b}{dr} \right)^2 + V(\phi_b, T) \right). \tag{4}$$

It is equivalent to the differential system

$$\frac{d^2\phi_b}{dr^2} + \frac{2}{r}\frac{d\phi_b}{dr} - \frac{\partial V}{\partial \phi_b} = 0, \quad \text{with} \quad \left.\frac{d\phi_b}{dr}\right|_{r=0} = 0 \ \text{ and } \ \phi_b|_{r=\infty} = 0, \tag{5}$$

that can be solved using an overshooting–undershooting method. The phase transition completes when the probablility for the nucleation of 1 bubble per 1 horizon volume is of order 1, which translates into the condition

$$S_3(T_\star)/T_\star \sim 140. \tag{6}$$

4 Estimate of the GW energy density

The energy density in gravitational waves coming from bubble collision can be estimated by naive dimensional analysis as follows. The quadrupole formula for the power of gravitational emission is $P_{GW} = \frac{G}{5}\langle (\dddot{Q}_{ij}^{TT})^2 \rangle$ where G is the Newton's constant and Q_{ij}^{TT} is the quadrupole moment of the source which is T_{ij}^{TT}, the transverse traceless piece of the stress tensor. We can write

$$\dddot{Q}_{ij}^{TT} \sim \frac{\text{mass of system in motion} \times (\text{size of system})^2}{(\text{time scale of system})^3} \sim \frac{\text{kinetic energy}}{\text{time scale of system}}. \tag{7}$$

thus, $P_{GW} \sim G\dot{E}_{kin}^2$. Let κ be the efficiency factor which quantifies the fraction of the vacuum energy which goes into kinetic energy of bulk motions of the fluid (as opposed to heating):

$$E_{kin} \sim \kappa \ \alpha \ \rho_{rad} \ (v_b \beta^{-1})^3. \tag{8}$$

Using $G \sim H_*^2/\rho_{tot*}$ and $\rho_{tot*} = (1+\alpha)\rho_{rad}$ we get

$$\Omega_{GW*} = \frac{\rho_{GW*}}{\rho_{tot*}} \sim \left(\frac{H_*}{\beta} \right)^2 \kappa^2 \frac{\alpha^2}{(1+\alpha)^2} v_b^3. \tag{9}$$

This is the energy density at the time of emission. To obtain the energy density today, we need to appropriately redshift it. We work in a standard Friedman–Robertson–Walker (FRW)

cosmology, $a(t)$ is the cosmological scale factor. At the energy scales considered, we assume a radiation-dominated era. Gravity waves produced at T_* with a characteristic frequency f_* propagate until today without interacting. Their energy density redshifts as a^{-4} and their frequency as a^{-1}. The characteristic frequency we observe today is

$$f = f_* \frac{a_*}{a_0} = f_* \left(\frac{g_{s0}}{g_{s*}}\right)^{1/3} \frac{T_0}{T_*}. \tag{10}$$

Today, $g_s(T_0) \simeq 3.91$ (assuming three neutrino species) and $T_0 = 2.725K = 2.348 \times 10^{-13}$ GeV. It is convenient to express the frequency in terms of the Hubble frequency at the time of GW production:

$$f \approx 6 \times 10^{-3}\text{mHz} \left(\frac{g_*}{100}\right)^{1/6} \frac{T_*}{100\text{GeV}} \frac{f_*}{H_*}. \tag{11}$$

And the fraction of the critical energy density in gravity waves today is

$$\Omega_{GW} = \frac{\rho_{GW}}{\rho_c} = \Omega_{GW*} \left(\frac{a_*}{a_0}\right)^4 \left(\frac{H_*}{H_0}\right)^2 \simeq 1.67 \times 10^{-5} h^{-2} \left(\frac{100}{g_*}\right)^{1/3} \Omega_{GW*}. \tag{12}$$

g_* is the number of relativistic degrees of freedom at T_* which enters the definition of the energy density and not the entropy. Ω_{GW*}, estimated in Eq. (9), is the fraction of energy density of the universe at the time of the transition which is in gravitational waves. To obtain an observable signal today, Ω_{GW*} had to be quite big: The peak sensitivity of LISA would correspond to detect $\Omega_{GW} h^2 \sim 10^{-11}$. This means that to detect a signal at LISA, we need $\Omega_{GW*} \gtrsim 10^{-6}$ while at BBO, we can probe smaller fractions, $\Omega_{GW*} \sim 10^{-12}$–$10^{-9}$.

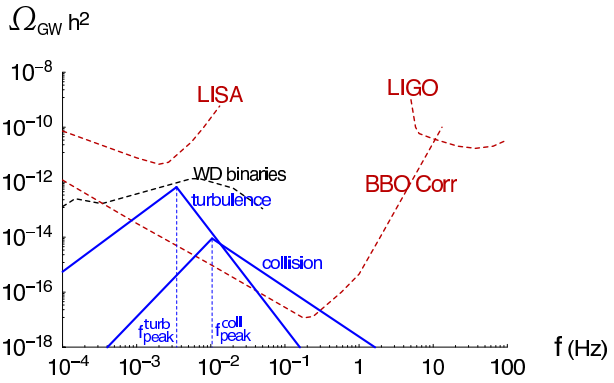

Figure 1: GW background created by collision and turbulence effect during a first-order phase transition at $T = 100$ GeV (for $\alpha = .8$ and $\beta/H = 2000$). The collision spectrum raises like $f^{2.8}$ and falls like $f^{-1.8}$ around the peak. The turbulence spectrum raises like f^2 and falls like $f^{-7/2}$. The full expressions for the peak frequencies as well as the GW energy density at the peaks can be found in [1, 7]. The turbulence peak always appears at lower frequency than the collision peak. The dashed rad lines are the (approximate) predicted sensitivities of LISA, BBO and LIGO-III. The black dashed curve is the estimate for the irreducible foreground due to white dwarf binaries.

5 Scanning the (α, β/H_*) plane

The GW background from first-order phase transition is the superposition of the collision and turbulence signals. We compare the GW spectra resulting from PT occurring at temperatures in the range [100 GeV, 100 PeV] with the sensitivities of LISA, BBO and LIGO correlated third

generation. For each temperature, we are making a full scan of the (α, β/H_*) parameter space and determine the regions where at least one of the peaks is observable. Various situations can arise (see Fig. 2):

- For relatively low α, the turbulence and collision peaks are well separated and can be observed. This is the ideal situation as the observability of these two peaks would be a smoking gun for the phase transition origin of these GW. The ratio of the two peak frequencies is a predicted function of α. In somes cases, the turbulence peak is at too low frequency to be observed by LISA or BBO but the minimum separating the two peaks is visible.

- At larger α ($\gtrsim 0.64$), the collision peak is hidden by the high frequency tail of the turbulence peak. However, there is a characteristic change of slope in the high frequency tail. Depending on the temperature of the transition, this change of slope can be observed or not.

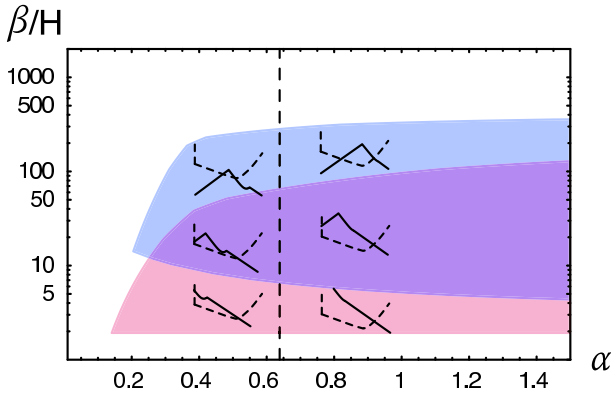

Figure 2: Different configurations of the signal versus the instrument sensitivity to show the qualitative dependence on parameters. The upper blue region is where the turbulence peak is observable while the lower red one is the region where either the collision peak or the point of slope change is visible. Precise locations of these different regions depend on the experiment and the temperature of the transition as illustrated in Figs. 3.

The full detectability plots can be found in our paper [1]. In Fig. 3, we just give examples of detectability by LISA and BBO of a phase transition taking place at $T = 500$ GeV. LISA could be sensitive to phase transitions taking place in the 50 GeV–100 TeV temperature range. An example of a potentially strong signal is provided by the Randall–Sundrum phase transition [8]. LIGO and BBO could be sensitive up to 10^7 GeV.

Notice also, as illustrated in Fig. 4, that GW signal from phase transition at around 10–100 TeV temperatures could entirely screen the signal from inflation, which detection is one of the main motivations for building BBO.

6 GW in a model with a H^6 potential

In the Standard Model, a first-order phase transition could in principle occur due to thermally generated cubic Higgs interactions

$$V(\phi, T) \simeq \frac{1}{2}\left(-\mu_h^2 + cT^2\right)\phi^2 + \frac{\lambda}{4}\phi^4 - ET\phi^3, \tag{13}$$

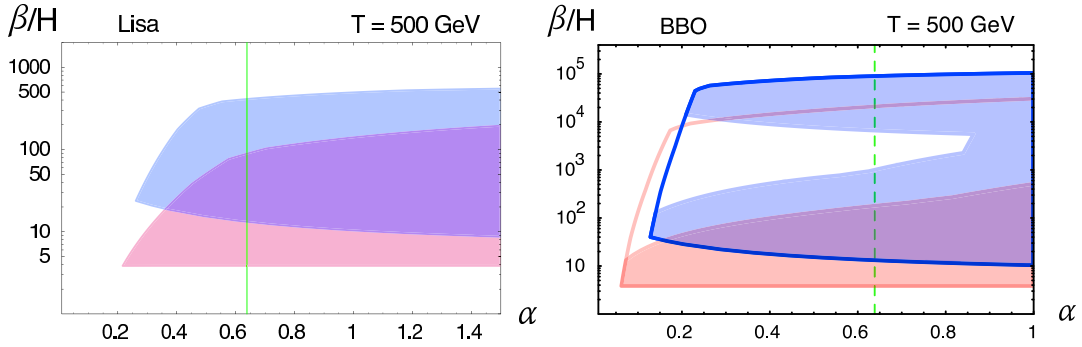

Figure 3: Contours delimiting the region in the $(\alpha, \beta/H)$ plane for which there is an observable peak at LISA (left figure) and at BBO (right figure). The upper blue region is for the turbulence peak while the lower red one is the region where either the collision peak or the point of slope change is visible. Left of the vertical green line, the collision peak is visible. The effect of including the constraint from the irreducible WD foreground is displayed and, at BBO, limits the observable regions from the uncolored ones to the ones in plain colors. As the temperature increases, the peaks are shifted to higher frequencies, thus the effect of the WD foreground becomes less significant.

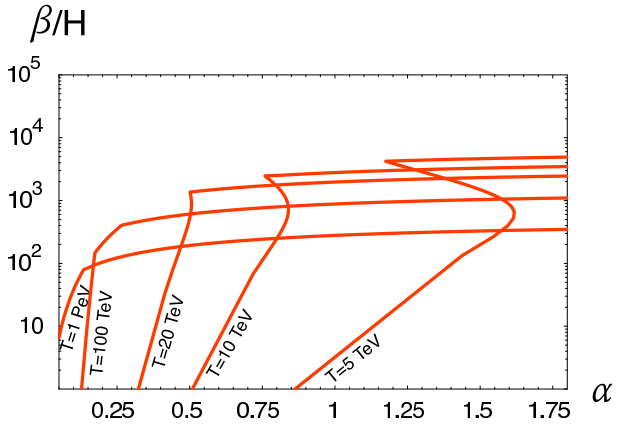

Figure 4: Below each line associated with the temperature of the phase transition, the gravitational wave signal at BBO from first-order phase transitions entirely masks the signal expected from inflation. This plot strongly depends on the scale of inflation, which was chosen here to be $E_I = 3.4 \times 10^{16}$ GeV.

with $E = \frac{4m_W^3 + 2m_Z^3}{12\pi v_0^3} \sim 6{\cdot}10^{-3}$. The strength of the phase transition is thus inversely proportional to the Higgs mass

$$\frac{\langle\phi(T_c)\rangle}{T_c} = \frac{4Ev_0^2}{m_h^2}. \tag{14}$$

Given the lower bound on the Higgs mass from LEP, the phase transition cannot be first order within the SM.

Higher-dimensional self-interactions can significantly affect the dynamics of the phase transition [9] (see also [10] and references therein). For instance a simple H^6 interaction in the Higgs potential

$$V(\phi) = \mu_h^2|H|^2 - \lambda|H|^4 + \frac{|H|^6}{\Lambda^2} \tag{15}$$

can induce a strong first-order phase transition if $\Lambda \sim 1$ TeV even for Higgs mass up to 200 GeV

(see Fig. 5). The H^6 interaction generates large deviations in the Higgs self-couplings when expanding around the vacuum (see Fig. 5)

$$\mathcal{L} = \frac{1}{2}m_h^2 h^2 + \frac{\mu}{6}h^3 + \frac{\eta}{24}h^4 + \cdots \tag{16}$$

with

$$\mu = 3\frac{m_h^2}{v_0} + 6\frac{v_0^3}{\Lambda^2}, \text{ and } \eta = 3\frac{m_h^2}{v_0^2} + 36\frac{v_0^2}{\Lambda^2}. \tag{17}$$

Precise measurements of the Higgs self-interactions at colliders are certainly a good place to test the presence of the H^6 interaction, even though these measurements are notoriously difficult and would have to wait for a fully operational Linear Collider. Meanwhile, the H^6 effects on the dynamics of the phase transition and the production of GW can be looked for with LISA and BBO. Fig. 6 shows for instance some contour plots of the quantity α in the plane (m_h, Λ).

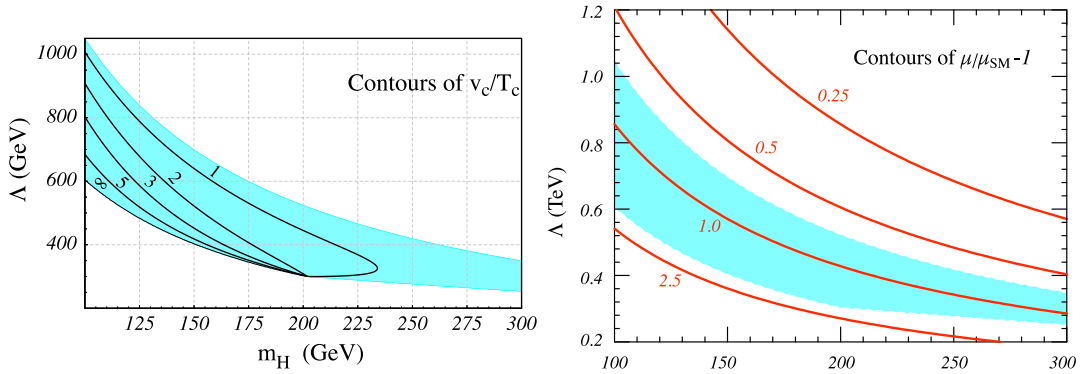

Figure 5: (Left) Contours of ϕ_c/T_c in presence of H^6 interaction in the Higgs potential: a strong first-order phase transition can be obtained even for Higgs mass as large as 200 GeV. In the shaded blue region, the phase transition is first-order. (Right) Deviations in the Higgs cubic self-interactions compared to the SM value.

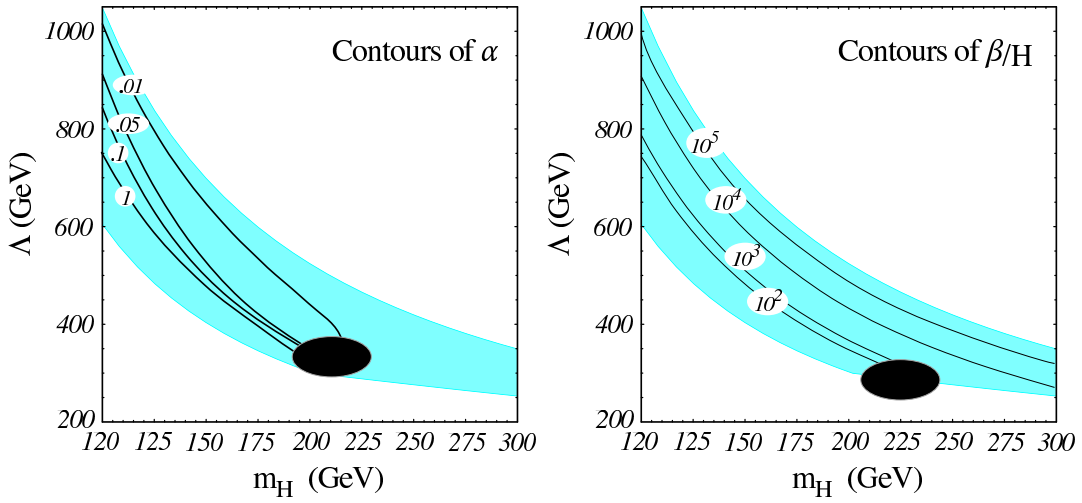

Figure 6: Contours of the quantities α (Right) and β/H (Left) in the plane (m_h, Λ) in presence of H^6 interaction in the Higgs potential. The black ellipses delineate regions where our numerical procedure failed to converge.

7 Conclusion

The GW background from early universe phase transitions may become relevant for GW detectors. LISA, LIGO and BBO will be able to probe part of the history of the universe in the temperature range 100 GeV–10^7 GeV. The GW signal coming from particle physics phase transitions is directly related to the scalar potential describing the evolution of the order parameter. Observation or non-observation of GW will allow to put constraints on the parameters of these potentials. The measurement of the GW spectrum (peak frequency and intensity) can discriminate among different models and put constraints on the model parameters. For example, at LHC, we will be able to measure the Higgs mass but not the quartic or cubic self coupling of the Higgs. Only a linear collider can provide this information, which timescale could be beyond LISA. LISA could start constraining model parameters before a linear collider. So we might well learn something about the Higgs by looking at the sky!

Acknowledgments

C.G. would like to thank the organizers of Quarks'06 and SUSY'06 for their kind invitations. This work is supported in part by the RTN European Program MRTN-CT-2004-503369, by the ACI Jeunes Chercheurs 2068 and by CNRS/USA exchange program PICS 3503.

References

[1] C. Grojean and G. Servant, arXiv:hep-ph/0607107.

[2] C. J. Hogan, arXiv:astro-ph/9809364.

[3] A. Kosowsky, M. S. Turner and R. Watkins, Phys. Rev. Lett. **69**, 2026 (1992), and Phys. Rev. D **45**, 4514 (1992). A. Kosowsky and M. S. Turner, Phys. Rev. D **47**, 4372 (1993) [arXiv:astro-ph/9211004]. M. Kamionkowski, A. Kosowsky and M. S. Turner, Phys. Rev. D **49**, 2837 (1994) [arXiv:astro-ph/9310044].

[4] K. Kajantie, M. Laine, K. Rummukainen and M. E. Shaposhnikov, Phys. Rev. Lett. **77**, 2887 (1996); K. Rummukainen, M. Tsypin, K. Kajantie, M. Laine and M. E. Shaposhnikov, Nucl. Phys. B **532**, 283 (1998); F. Csikor, Z. Fodor and J. Heitger, Phys. Rev. Lett. **82**, 21 (1999).

[5] A. Kosowsky, A. Mack and T. Kahniashvili, Phys. Rev. D **66**, 024030 (2002) [arXiv:astro-ph/0111483]. A. D. Dolgov, D. Grasso and A. Nicolis, Phys. Rev. D **66**, 103505 (2002) [arXiv:astro-ph/0206461].

[6] R. Apreda, M. Maggiore, A. Nicolis and A. Riotto, Nucl. Phys. B **631**, 342 (2002) [arXiv:gr-qc/0107033].

[7] A. Nicolis, Class. Quant. Grav. **21**, L27 (2004) [arXiv:gr-qc/0303084].

[8] L. Randall and G. Servant, arXiv:hep-ph/0607158.

[9] C. Grojean, G. Servant and J. D. Wells, Phys. Rev. D **71**, 036001 (2005) [arXiv:hep-ph/0407019].

[10] S. J. Huber, M. Pospelov and A. Ritz, arXiv:hep-ph/0610003.